ORIGINAL RESEARCH

RTP801 Amplifies Nicotinamide Adenine Dinucleotide Phosphate Oxidase-4–Dependent Oxidative Stress Induced by Cigarette Smoke

Daniel Hernández-Saavedra[1,2], Linda Sanders[1], Mario J. Perez[1], Beata Kosmider[3], Lynelle P. Smith[1], John D. Mitchell[4], Toshinori Yoshida[5], and Rubin M. Tuder[1]

[1]Program in Translational Lung Research, Division of Pulmonary Sciences and Critical Care Medicine, [2]Cardiovascular Pulmonary Research Laboratories, Department of Pediatrics, and [4]Department of Surgery, Division of Cardiothoracic Surgery, University of Colorado School of Medicine, Anschutz Medical Campus, Aurora, Colorado; [3]Department of Medicine, National Jewish Health, Denver, Colorado; and [5]Laboratory of Veterinary Pathology, Tokyo University of Agriculture and Technology, Tokyo, Japan

Abstract

Tobacco smoke (TS) causes chronic obstructive pulmonary disease, including chronic bronchitis, emphysema, and asthma. Rtp801, an inhibitor of mechanistic target of rapamycin, is induced by oxidative stress triggered by TS. Its up-regulation drives lung susceptibility to TS injury by enhancing inflammation and alveolar destruction. We postulated that Rtp801 is not only increased by reactive oxygen species (ROS) in TS but also instrumental in creating a feedforward process leading to amplification of endogenous ROS generation. We used cigarette smoke extract (CSE) to model the effect of TS in wild-type (Wt) and knockout (KO-Rtp801) mouse lung fibroblasts (MLF). The production of superoxide anion in KO-Rtp801 MLF was lower than that in Rtp801 Wt cells after CSE treatment, and it was inhibited in Wt MLF by silencing nicotinamide adenine dinucleotide phosphate oxidase–4 (Nox4) expression with small interfering Nox4 RNA. We observed a cytoplasmic location of ROS formation by real-time redox changes using reduction-oxidation–sensitive green fluorescent protein profluorescent probes. Both the superoxide production and the increase in the cytoplasmic redox were inhibited by apocynin. Reduction in the activity of Sod and decreases in the expression of *Sod2 and Gpx1* genes were associated with Rtp801 CSE induction. The ROS produced by Nox4 in conjunction with the decrease in cellular antioxidant enzymatic defenses may account for the observed cytoplasmic redox changes and cellular damage caused by TS.

Keywords: Rtp801 cigarette smoke extract induction; nicotinamide adenine dinucleotide phosphate oxidase-4; oxidative stress

Tobacco smoke (TS) causes chronic obstructive pulmonary disease (COPD), which is the third leading cause of mortality in North America, and has a far-reaching impact worldwide. TS contains thousands of chemical compounds, many with potent oxidant capabilities (1). These oxidants trigger the production of reactive oxygen species (ROS), causing oxidative stress and leading to lung inflammation, which involves the recruitment of neutrophils, macrophages, and multiple lymphocyte populations, including TH17, natural killer, and cytotoxic lymphocytes. Over time, TS leads to remodeling of the pulmonary airway structures, which is characterized by airway inflammation, an increase in airway connective tissue, and mucus accumulation; these processes underlie the key manifestation of chronic bronchitis in COPD. COPD also includes emphysema characterized by alveolar destruction, causing a marked reduction in gas exchange area and ventilatory capacity. Emphysema involves a complex interplay of inflammation, excessive extracellular matrix proteolysis (performed by elastin-degrading proteases), and alveolar cell apoptosis and autophagy (2, 3). Finally, it has been recognized that emphysema caused by TS involves accelerated aging, with increased expression of markers of cellular senescence and decreased telomere length and

(Received in original form May 6, 2016; accepted in final form August 12, 2016)

This work was supported by National Institutes of Health Grants R01 ES016285 (R.M.T.), 2 T32 HL007171 (D.H.-S.), and R01 HL118171, and by Flight Attendant Medical Research Institute, Inc. (Clinical Innovator Award) (B.K.).

Author Contributions: Conception and design: D.H.-S. and R.M.T.; analysis and interpretation: D.H.-S., L.S., M.J.P., B.K., L.P.S., J.D.M., T.Y., and R.M.T.; drafting of the manuscript and review for important intellectual content: D.H.-S. and R.M.T.

Correspondence and requests for reprints should be addressed to Rubin M. Tuder, M.D., Program in Translational Lung Research, Division of Pulmonary Sciences and Critical Care Medicine, University of Colorado School of Medicine, Anschutz Medical Campus, Research 2–9th floor; Mail stop C-272, 12700 East 19th Avenue, Aurora, CO 80045. E-mail: rubin.tuder@ucdenver.edu

This article has an online supplement, which is accessible from this issue's table of contents at www.atsjournals.org

Am J Respir Cell Mol Biol Vol 56, Iss 1, pp 62–73, Jan 2017

Originally Published in Press as DOI: 10.1165/rcmb.2016-0144OC on August 24, 2016
Internet address: www.atsjournals.org

telomerase activity (4), all of which can increase susceptibility to lung destruction by TS (1).

Although lung diseases caused by TS have long been ascribed to oxidative stress, the first conclusive demonstration of the role of oxidative stress in COPD originated from data in mice deficient in the master antioxidant transcription factor, nuclear erythroid-related factor 2 (Nrf-2) (5). Nrf-2 regulates several of the key antioxidant genes, including that encoding glutathione peroxidase (Gpx), and several of the gene products involved in glutathione synthesis (6). Nrf-2 knockout mice developed more severe and earlier alveolar inflammation, cell death, and ultimately emphysema than did wild-type (Wt) littermate control mice.

We hypothesized that TS triggers cellular responses akin to those of environmental stresses (7) such as hypoxia, nutrient deprivation, or radiation. The sensing of these stress cues converges at the mechanistic target of rapamycin (mTOR). mTOR is an important regulator of cell growth, messenger RNA (mRNA) translation, and activation of anabolic processes (8). We have shown that Rtp801 (also known as DDIT4 for DNA damage inducible transcript, Dig2 for dexamethasone inducible gene, or REDD1 for regulated in development and DNA damage responses) drives lung susceptibility to TS, leading to inflammation and alveolar destruction (9). Rtp801 is induced by oxidative stress triggered by TS (9), leading to mTOR inhibition caused by the activation of Tsc2. Rtp801 binds to Tsc2, displacing the adaptor 14-3-3 protein (10). Although we did not observe down-regulation of Nrf-2 or its target genes because of Rtp801 overexpression (T. Yoshida and R. M. Tuder, unpublished observations), Nrf-2 knockout mice had increased lung Rtp801 expression when exposed to TS, as compared with Wt mice (9). Importantly, we found that RTP801 expression was increased in the lungs of patients with COPD who were exposed to TS (9), underscoring its potential role in COPD pathogenesis.

We postulated that the Rtp801expression is not only induced by ROS in TS, but also instrumental in creating a feedforward process leading to amplification of endogenous ROS generation. Furthermore, we investigated the location and type of ROS produced when cells were exposed to TS. In aggregate, this investigation provides novel insights into how the Rtp801/mTOR axis enhances the underlying mechanisms involved in TS-induced oxidative stress and ensuing injury. We used mouse lung fibroblasts (MLF) as a model system because they undergo several

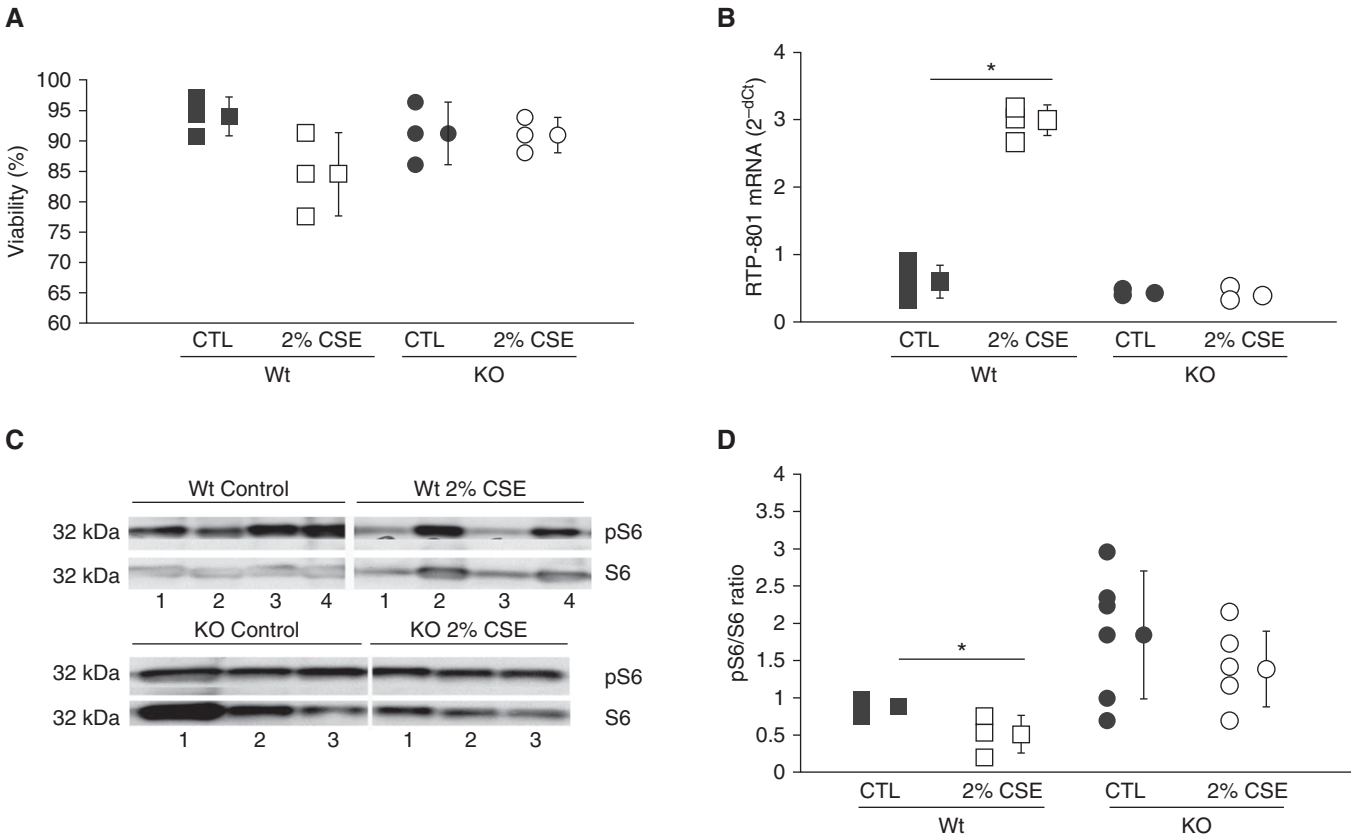

Figure 1. Cigarette smoke extract (CSE) induces Rtp801 overexpression and diminishes the viability of mouse lung fibroblasts (MLF). (*A*) Wild-type (Wt) ($n = 3$) and knockout (KO) Rtp801 (KO-Rtp801) ($n = 3$) MLF (10^5) were exposed to 2% CSE for 4 hours, and the viability was assessed by trypan blue exclusion. (*B*) Rtp801 mRNA overexpression in MLF after incubation for 4 hours in 2% CSE (Wt, $n = 4$; KO-Rtp, $n = 3$). (*C*) Western blot analysis of S6 phosphorylation (pS6) in Wt ($n = 6$, 4 shown) and KO-Rtp801 ($n = 6$, 4 shown) MLF after 4 hours of 2% CSE treatment. (*D*) Densitometric analysis of the Western blot. Data represent the average of at least three independent experiments performed in triplicate, and *error bars* indicate SDs. Kruskal–Wallis significance, $^*P \leq 0.001$ (Wt: CTL versus 2% CSE, Figure 1B). ANOVA, $^*P \leq 0.05$ for *D*. CTL, control.

pathogenic processes similar to those of the type I, type II, and endothelial cells in the COPD lung (11).

Materials and Methods

Medium and reagents suppliers are available in the online supplement; the xanthine oxidase was obtained from milk as described by Waud (12).

Cell Lines and Cell Cultures

Primary MLF were purified from Wt, Rtp801 knockout (KO-Rtp801), and Rtp801 overexpressing (Tg-TRE-RTP801) mice whole lungs and were cultured as described (*see* online supplement). Primary human alveolar type II (ATII) cells were isolated and maintained in their differentiated state (13, 14). Cigarette smoke treatment and cell viability were assessed (*see* online supplement).

Cytochrome *c* Reduction Assay

The production of the superoxide was quantified by the reduction of cytochrome *c* (*see* online supplement).

Mitochondrial-Superoxide Production

MLF were preincubated for 10 minutes with 5 μM MitoSOX Red, and the fluorescence was recorded in a plate reader (*see* online supplement).

Nicotinamide Adenine Dinucleotide Phosphate–Superoxide Production Inhibition

One hundred micromolars of apocynin was used, and the amount of superoxide was estimated using MitoSOX Red or cytochrome *c* reduction as above.

Gene Expression

The expression of genes in the MLF samples after cigarette smoke extract (CSE) treatment was assessed by quantitative reverse transcriptase polymerase chain reaction (*see* online supplement).

Sod, Catalase, and Glutathione Peroxidase Activity Assays

Sod activity was measured using the cytochrome *c* reduction inhibition assay as described by McCord and Fridovich (15). Catalase activity was evaluated according to Bergmeyer (16). Gpx enzymatic activity was evaluated according to Lawrence and Burk (17). The protein content of crude extracts

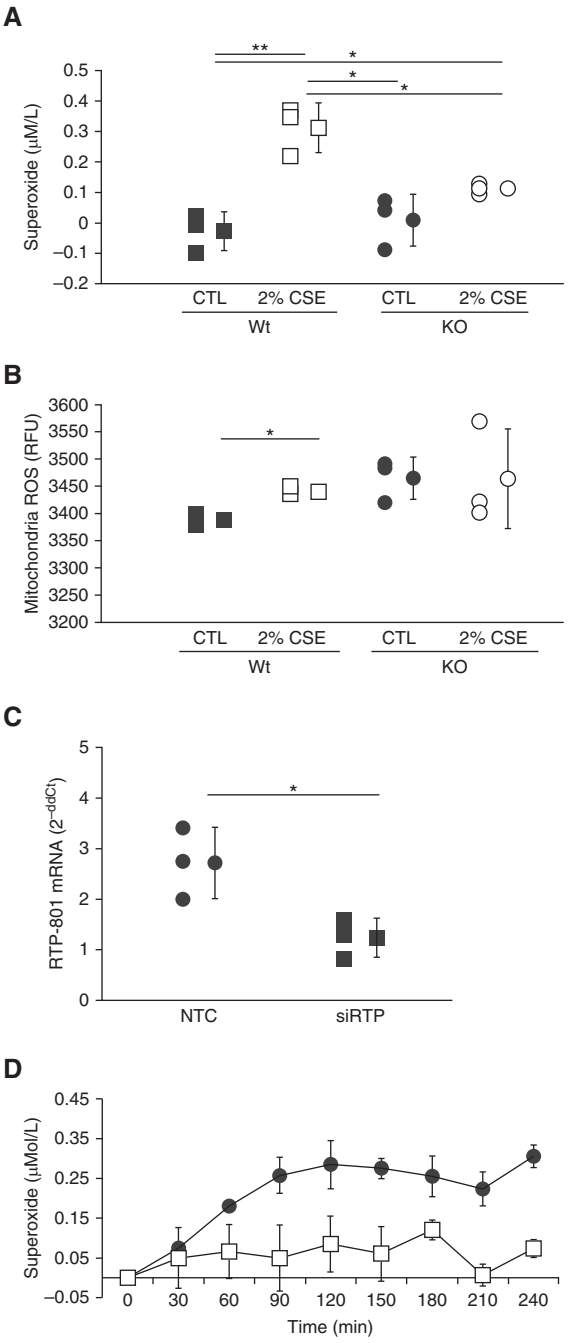

Figure 2. Production of superoxide radical ($O_2^{\cdot-}$) is lower in KO-Rtp801 MLF after CSE treatment. (*A*) Total superoxide production in Rtp801 Wt MLF ($n = 3$) and KO-Rtp801 ($n = 3$) growing cells under 2% CSE incubation (60 min) measured by cytochrome *c* reduction assay inhibitable by superoxide dismutase. (*B*) Mitochondrial superoxide formation after 2% CSE incubation of Wt MLF ($n = 3$) and KO-Rtp801 ($n = 3$) as determined by the relative emission of fluorescence using MitoSOX Red mitochondrial probe. (*C*) Rtp801 relative gene expression ($2^{-\Delta\Delta Ct}$) in MLF Wt cells treated with small interfering Rtp801 (siRtp801) RNA ($n = 3$), and scrambled small interfering RNA as negative control ($n = 3$). (*D*) Superoxide production in MLF transfected with siRtp801 RNA (*open squares*, $n = 3$) when compared with scrambled RNA control (*solid circles*, $n = 3$) as determined by the cytochrome *c* reduction assay as before. Data represent the average of at least three independent experiments performed in triplicate, and *error bars* indicate SD. Kruskal–Wallis significance, $^*P \leq 0.05$ or $^{**}P \leq 0.001$ for *A* to *C*. ANOVA, $^*P \leq 0.05$ or $^{**}P \leq 0.001$, and Student's two-tailed *t* test, $^*P \leq 0.05$ against untreated control cells in *D*. ROS, reactive oxygen species; RFU, relative fluorescence units. NTC, no template control.

was measured using the method described by Lowry and colleagues (18).

Activity Gels

Concentrated supernatants containing 0.05 U of Sod activity were separated electrophoretically, and the gel was stained for activity with Nitroblue tetrazolium-riboflavin-Ethylenediaminetetraacetic and then developed under fluorescent light.

Glutathione Determination

MLF cell suspensions were used for glutathione determination using the Elite Glutathione GSH/GSSG Ratio Assay following the manufacturer's instructions (eENZYME, LLC, Gaithersburg, MD).

Western Analysis

Proteins were separated by electrophoresis and then transferred onto membrane and blocked in 5% bovine serum albumin–Tris-Buffered Saline Tween. Membranes were incubated with primary antibodies at 4°C overnight and with HRP-labeled goat antirabbit secondary antibody for 1 hour and were detected using enhanced chemiluminescence (*see* online supplement).

Gene Silencing

One hundred nanomolars of small interfering nicotinamide adenine dinucleotide phosphate (NADPH) oxidase–4 (Nox4) (siNox4) (sense or antisense custom oligos), 10 nM of siNox4, 10 nM of siTsc2 (Ambion, Carlsbad, CA), or 1 μM of Accell siRTP801 mix (GE Dharmacon, Buckinghamshire, UK) were used in Accell Delivery Media, and the expression and superoxide production were assessed (*see* online supplement). Silenced MLF with siNOX4 (Ambion) or Accell siRTP801 mix were disrupted and used for glutathione determination.

Real-Time Redox Sensing

MLF were transduced with 200 plaque-forming units per cell of the adenovirus targeted to mitochondria (Mito-reduction-oxidation [ro]–sensitive green fluorescent protein [GFP]) or cytoplasm (Cyto-roGFP). The fluorescence of CSE-treated MLF was recorded (*see* online supplement), and calculations were performed as described by Waypa and Schumacker (19).

Rtp801 Overexpression in MLF

We created Rtp801-overexpressing mice (Tg-TRE-RTP801) (20). TgRtp801 MLF were purified and cultured as described above. The induction of Rtp801 expression was performed by transduction with 100 plaque-forming units per cell of the transactivator tet-off tTA-adenovirus (or CMV-GFP-adenovirus as control). The expression of the transgene was confirmed via reverse transcriptase polymerase chain reaction, and we then monitored the superoxide production and gene expression (*see* online supplement).

Statistics

Data represent the average of at least three independent experiments, and *error bars* indicate SD. We performed parametric analysis with the Student's two-tailed *t* test when comparing two groups and one-way analysis of variance with Fisher *post hoc* testing when multiple comparisons were performed. Those experiments, with three to four independent experiments (performed in triplicate each), were analyzed with a more stringent nonparametric test (Kruskal–Wallis). Differences were statistically significant if $P \leqslant 0.05$ or $P \leqslant 0.001$, as indicated in the figures and legends. We performed all calculations using ProStat software (Pearl River, NY).

Results

Changes in Viability and Rtp801 Gene Expression after TS Treatment of MLF

During the gaseous phase, TS dissolves in media, forming CSE, which can be used to model the effect of TS at the extracellular lining fluid of the lung (21). CSE (2% in media, see METHODS) treatment for 4 hours diminished the viability of MLF (called here after Wt cells) (Figure 1A), whereas it induced Rtp801 expression, as we described previously (9) (Figure 1B). In contrast, MLF originating from KO-Rtp801 showed no changes in viability to CSE (Figure 1A). As anticipated on the basis of the known function of Rtp801 in suppressing mTOR (22), CSE-treated Wt MLF (2% for 4 h) showed a decrease in phosphorylated S6 in position Thr^{389} (9, 23), as assessed by densitometric analysis of Western blots of cell lysates (Figure 1D). As we have reported previously, KO-Rtp801 cells maintained their increased basal phosphorylated S6 levels after CSE (Figure 1C), which were higher than those detected in CSE-treated Wt MLF (9) (Figure 1D).These changes were not accompanied by changes in mTOR phosphorylation (data not shown).

Production of Superoxide Radical ($O_2^{\cdot-}$) in MLF after CSE Treatment

We first defined the time course of total superoxide production in Rtp801 Wt MLF when treated with 2% CSE by measuring cytochrome *c* reduction. There was a significant increase of superoxide in Wt cells at 60 minutes of incubation. However, CSE did not increase the levels of superoxide in KO MLF when compared with Wt MLF (Figure 2A). In line with these findings, the silencing of Tsc2 (a Rtp801 downstream inhibitor of mTOR activation) with small interfering RNA (siRNA) (*see* Figure E1 in the online supplement) showed superoxide production similar to that of KO-Rtp801 MLF (Figure 2A) after CSE treatment. As expected, we found mitochondrial superoxide formation after CSE incubation of MLF, but to a lesser extent, as determined by the relative emission of fluorescence using a MitoSOX Red mitochondrial probe (Figure 2B). We further preincubated the MLF with inhibitors of the mitochondrial electron chain transfer (antimycin, rotenone, and myxothiazol), as well as with the NADPH inhibitor apocynin, and found no significant inhibition on MitoSox Red florescence after CSE incubation (data not shown). These results were further confirmed by inhibiting the *Rtp801* gene expression with an siRNA in Wt cells (Figure 2C), which led to a significant decrease in the induction of superoxide anion after CSE treatment, with no changes when scrambled siRNAs were used as negative controls (Figure 2D). The reduced/oxidized glutathione ratio was evaluated in MLF after 2% CSE. The pools of GSH were not changed in the Wt MLF after CSE treatment; however, the siRtp801-treated Wt MLF showed an important increase in the GSH/GSSG ratio (Table 1). The aggregate of these findings indicates that CSE-induced Rtp801 leads to increased superoxide generation.

Table 1. GSH/GSSG Ratio in Wt, siRtp801, and siNox4 MLF after 2% CSE

Treatment	Wt	siRTP801	siNOX4
Control	1.10 ± 0.05	1.42 ± 0.56	0.89 ± 0.22
2% CSE	1.09 ± 0.14	1.94 ± 0.06	1.68 ± 0.09

Definition of abbreviations: CSE, cigarette smoke extract; GSH/GSSG, reduced/oxidized glutathione ratio; MLF, mouse lung fibroblasts; NOX4, nicotinamide adenine dinucleotide phosphate oxidase–4; si, small interfering; Wt, wild type.
Data represent one experiment per condition in triplicates each.

Production of Superoxide Radical by Nox4

MLF are known to particularly express Nox4, which produces ROS intra- and extracellularly (24). We determined the presence of the Nox4 isoform in the plasma membrane by cellular fractionation of Wt MLF. Figure 3A shows the Western blots of MLF cellular fractions: total cell membrane (organelle plus plasma membranes), purified plasma membrane, and cytosol, before and after CSE treatment. The Nox4 isoform, which was detected as a 61-kD band in total and plasma membrane fractions, strongly trended toward increased expression ($P = 0.058$) in MLF incubated 4 hours with 2% CSE versus controls. The total cell membrane and cytosolic fractions showed a strong band of ~90 kD, which may represent the highly stable Nox4/p22^{phox} heterodimer. The mRNA expression of Nox isoforms in MLF treated with 2% CSE showed a small, but not significant, increase in Nox4 expression in Wt MLF; in contrast, KO-Rtp801 MLF had a significant decrease in *Nox4* gene expression (Figure E2A). The levels of mRNA of the *Nox2* gene in both cell types were very low (10× compared

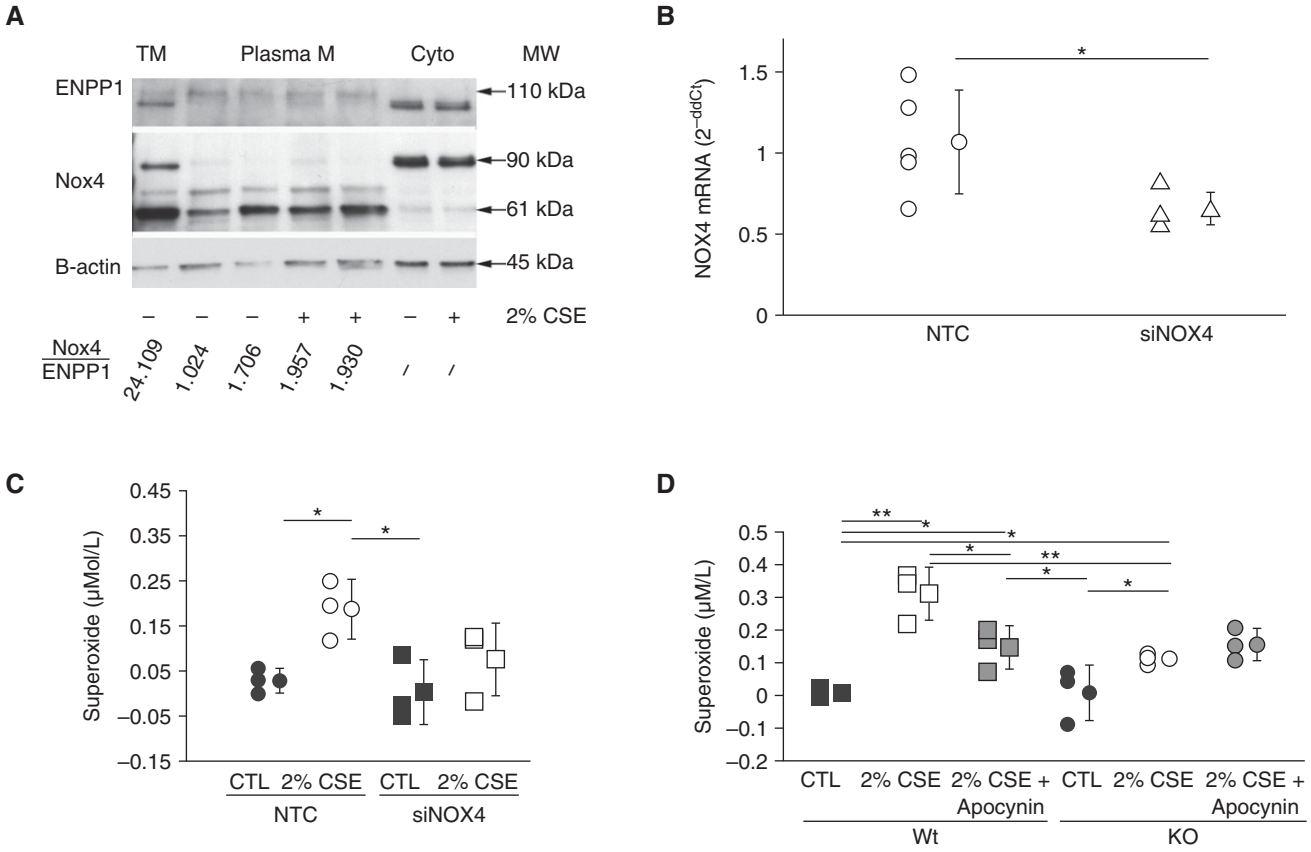

Figure 3. Nicotinamide adenine dinucleotide phosphate oxidase-4 (Nox4) is responsible for production of $O_2^{\cdot-}$ caused by CSE. (*A*) Localization of Nox4 by Western blot on cellular fractions (total membrane [TM], organelles and plasma membranes; plasma membrane [purified from total membrane]; and cytosol) of Wt Rtp801 MLF ($n = 2$); and ENPP1, a specific plasma membrane marker, and Nox4/β-actin ratios on the basis of electrophoretic density. β-actin was used as a protein loading control. The values represent two experiments per condition in triplicate each (plasma membrane statistical variation: control = 0.233, 2% CSE ⩽ 0.005). (*B*) 105 Wt MLF were transfected with NTC scrambled small interfering RNA (siRNA) ($n = 5$), and siNox4 ($n = 5$) and the relative expression ($2^{-\Delta\Delta Ct}$) of Nox4 gene measured after induction with 2% CSE. (*C*) Total superoxide production in NTC ($n = 3$) and siNox4 transfected Wt MLF ($n = 3$) after 2% CSE incubation (60 min) measured by cytochrome *c* reduction assay inhibitable by superoxide dismutase. (*D*) Superoxide production induced by CSE in Wt ($n = 3$) and KO-Rtp801 ($n = 3$) MLF cells inhibited by 30-minute preincubation with 100 mM apocynin ($n = 3$). Data represent the average of at least three independent experiments performed in triplicate, and *error bars* indicate SDs. ANOVA significance, $^*P \leqslant 0.05$ for *B*; Kruskal–Wallis significance, $^*P \leqslant 0.05$ or $^{**}P \leqslant 0.001$ for *C* and *D*. Cyto, cytoplasmic fraction; ENPP1, ectonucleotide pyrophosphatase-phospho-diesterase 1; MW, molecular weight.

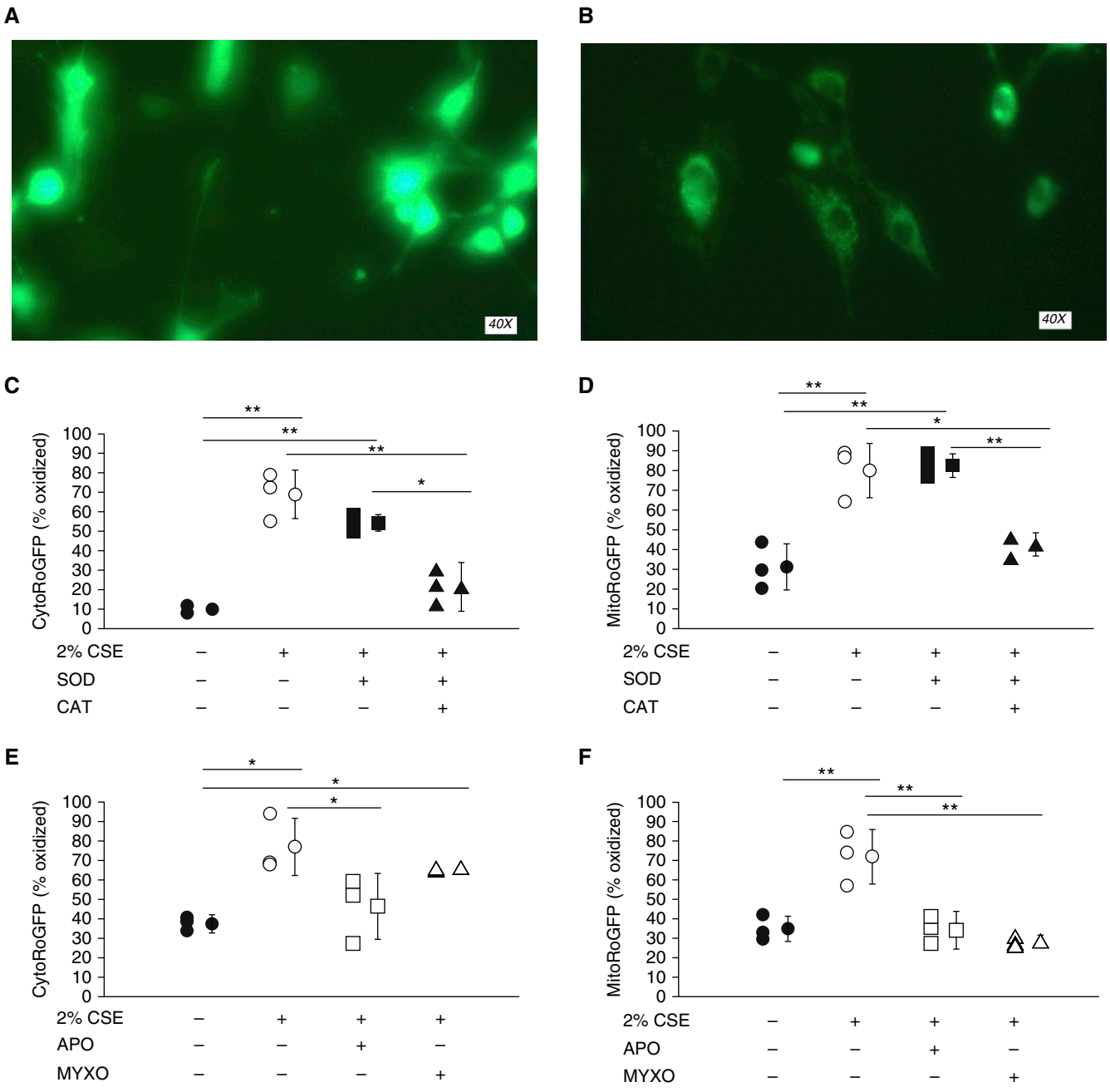

Figure 4. Cigarette smoke causes cytoplasmic oxidative stress in Wt MLF after 30 minutes. MLF transduced with (*A*) cytoplasm-reduction-oxidation (ro)–sensitive green fluorescent protein (GFP) (Cyto-roGFP) and (*B*) mitochondria-roGFP (Mito-roGFP) after CSE treatment. MLF (10^5) cells were transduced with redox-sensitive adenovirus encoding GFP probes targeting (*C*) the cytoplasm (Cyto-roGFP) or (*D*) the mitochondria (Mito-roGFP) and treated with 2% CSE (*open circles*, $n = 3$) or control (*solid circles*, $n = 3$) and in the presence of 6 U of hrSOD2 (SOD; *solid squares*, $n = 3$), or both, 6 U of hrSOD2, and 4 U of bovine catalase (CAT; *solid squares,* $n = 3$) antioxidant enzymes. (*E*) Cyto-roGFP MLF Wt transduced cells were treated with 2% CSE dimethyl sulfoxide (DMSO) (*open circles*, $n = 3$) or control DMSO (*solid circles*, $n = 3$) and in the presence of 100 mM apocynin (APO; *open squares*, $n = 3$) or 10 mM myxothiazol (MYXO; *open triangles*, $n = 3$). (*F*) Mito-roGFP MLF Wt transduced cells were treated with 2% CSE DMSO (*open circles*, $n = 3$) or control DMSO (*solid circles*, $n = 3$) and in the presence of 100 mM apocynin (*open squares*, $n = 3$) or 10 mM myxothiazol (*open triangles*, $n = 3$). The percentage of oxidized probe was determined by the ratio of reduced probe (measured with an excitation of 405 nm and emission of 535 nm) and oxidized probe (excitation of 485 nm and emission of 535 nm). Data represent the average of at least three independent experiments performed in triplicate, and *error bars* indicate SD. Kruskal–Wallis significance, $^*P \leq 0.05$ or $^{**}P \leq 0.001$. hrSOD2, human recombinant superoxide dismutase 2.

with Nox4), and their expression showed no changes after 4 hours of CSE treatment (Figure E2B). We inhibited *Nox4* gene expression by ~40–50%, with two different siRNAs (no template control scrambled and Tsc2 were used as negative siRNAs controls) (Figure 3B). After siRNA treatment, the Nox4 protein levels were reduced as well, although not significantly (data not shown). These decreased expressions may account for the observed reduction in superoxide, because only siNox4-treated MLF showed a significant decrease in superoxide levels after 2% CSE incubation (60 min) (Figure 3C), which persisted for >4 hours after TS treatment, as judged by the cytochrome *c* reduction inhibited by Sod (data not shown). In contrast, there was an increase in the pool of GSH after CSE exposure of siNOX4-treated MLF, as determined by the GSH/GSSG ratio (Table 1). MLF, transduced with control scrambled no template control, or siTsc2, remained capable of producing superoxide after CSE treatment (Figure 3C). To support these observations, we further inhibited the superoxide production induced by CSE by preincubating MLF with 100 μM apocynin, a NADPH oxidase (Nox) inhibitor. Only the Wt MLF treated with apocynin showed a significant inhibition of superoxide after CSE incubation. In contrast, the KO-Rtp801 MLF had no changes (Figure 3D).

Cytoplasmic Location of ROS Formation by Real-Time Redox Changes Using roGFP Profluorescent Probes

Because of the impact of cysteine oxidation on their fluorescent properties, GFP probes detect real-time redox changes. The fluorescence signal ultimately reflects the cellular GSH/GSSG ratio, on the basis of the preferential depletion of GSH potential caused by hydrogen peroxide, which is cell permeable. MLF Wt cells transduced with the redox-sensitive adenovirus encoding the GFP probe targeting the cytoplasm (Cyto-roGFP) showed a significant increase in florescence when exposed to CSE, as compared with untreated cells (Figures 4A and 4C). The cells transduced with the probe targeting the mitochondria (Mito-roGFP) also showed an increase in fluorescence with CSE, but it was not as pronounced as that observed with the Cyto-roGFP–transduced cells, given the higher baseline levels in the Mito-roGFP used (Figures 4B and 4D). Apocynin (100 μM) inhibited cytoplasmic ROS fluorescence production triggered by CSE in Wt cells (Figure 4E), with no differences when the cells were incubated with 10 μM of myxothiazol (a mitochondrial electron chain transfer complex III inhibitor). In addition, the oxidation of the roGFP mitochondrial probe was decreased when the transduced cells were treated with CSE in the presence of apocynin or myxothiazol (Figure 4F). When antioxidant enzymes were used extracellularly, we observed a decrease of fluorescence in both compartments when catalase was used (Figures 4C and 4D). The extracellular addition of human recombinant SOD2 showed no changes in the mitochondrial redox status (Figure 4D) and a light, nonsignificant inhibition of oxidation of the cytoplasmic roGFP probe (Figure 4C).

Antioxidant Enzymes Associated with Rtp801 CSE Induction

Table 2 and Figure 5 summarize the effect of CSE on antioxidant activity/expression in MLF after 4 hours of CSE treatment. In summary, CSE decreased Sod, whereas it minimally increased Gpx enzymatic antioxidant activities; it decreased *Sod2*, *Gpx1*, and *Prdx1* and increased *Sod3* gene expression in Wt MLF. We found significantly lower Sod1 and increased Gpx activities, as well as a significant increase of *Prdx1* expression in KO-Rtp801 cells after CSE incubation.

To further validate the role of Rtp801 in the enhancement of the oxidative stress triggered by TS, we overexpressed the *Rtp801* transgene (*TgRtp801*) in MLF to test whether its overexpression recapitulates the effects downstream of TS (without the potential confounding effects of lingering oxidants caused by TS in the media). The induction of *Rtp801* with the transactivator (AdtTA) caused overexpression of *Nox4* (Figure 6A), accompanied by increased levels of extracellular superoxide (Figure 6B). On the other hand, no changes in superoxide production were detected in mitochondria, as determined by MitoSOX Red (Figure 6C). The transactivation of the *TgRtp801* in MLF induced a decrease in the expression of the antioxidant enzymes *Sod2* and *Gpx1* (Figure 6D), similar to that which was observed with the CSE treatment of Wt MLF.

RTP801 and Antioxidant Enzyme Expression in Human ATII Cells and Lungs

To enhance the relevance of our findings, we extended our studies to human ATII cells isolated from the lungs of patients with COPD, smokers without COPD, and nonsmokers, which retain the molecular characteristics of the lungs in each of these groups. We found a significant increase in *RTP801* gene expression in human ATII cells (from nonsmokers) after 3% CSE treatment (one-half of the concentration used to assess cellular injury determined by prior studies [25]) (Figure 7A). In contrast to MLF, human type II cells showed an increase in *SOD2* expression, as well as diminished catalase expression (Figure 7A). There was a reduction in *GPX1* gene expression in primary human ATII cells after treatment with 3% CSE for 4 hours,

Table 2. Antioxidant Enzyme Activities and Gene Expression in Wt and KO-RTP801 Mouse Lung Fibroblasts

	Wt (2% CSE versus Ctl)		KO-Rtp801 (2% CSE versus Ctl)	
Enzyme	**Enz. Activity**	**Expression**	**Enz. Activity**	**Expression**
Total Sod	↓↓*	NA	↓↓*	NA
Sod1	↓↓↓	↑	↓↓↓*	↑
Sod2	↓↓*	↓↓*	↑	↓
Sod3	↑	↑*	ND	↓
Cat	↓↓	↑	↓	↑
Gpx	↑	↓*	↑*	↑
Prdx1	ND	↓*	ND	↑*

Definition of abbreviations: Cat, catalase; CSE, cigarette smoke extract; Ctl, control; Enz., enzyme; Gpx, glutathione peroxidase; KO, knockout; NA, does not apply; ND, not determined; Prdx1, peroxiredoxin-1; Sod, superoxide dismutase; Wt, wild type.
Changes after treatment with 2% CSE for 4 hours versus control. Kruskal–Wallis analysis.
*$P \leq 0.05$ against control cells.

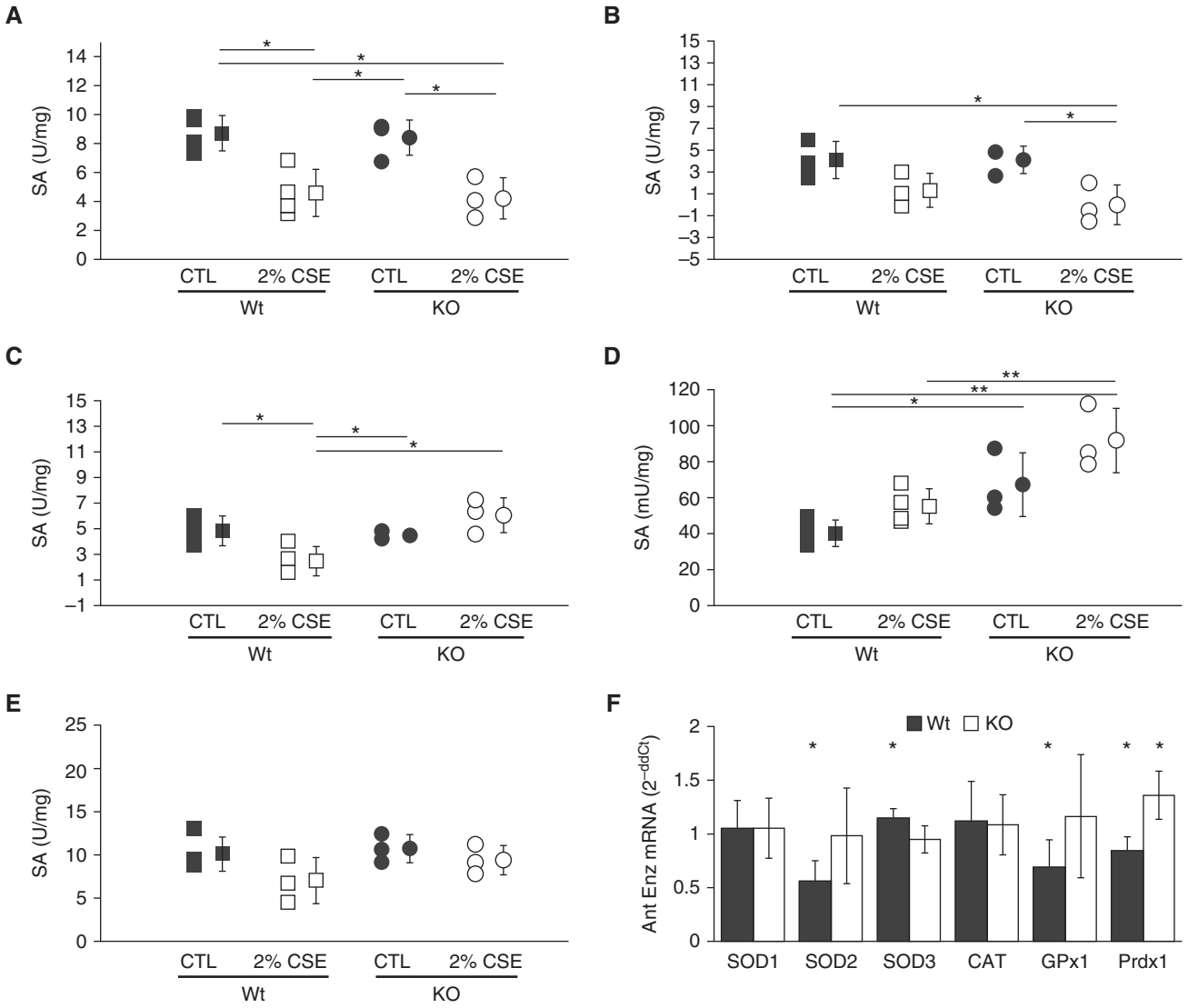

Figure 5. Cigarette smoke decreases Sod, whereas it minimally induces glutathione peroxidase (Gpx) enzymatic antioxidant activity with a selective inhibition of Sod2, Gpx1, and Prdx1 gene expression in Wt MLF. (*A*) Total Sod-specific enzymatic activity in cell lysates of Wt MLF ($n = 4$) and KO-Rtp801 ($n = 3$) treated with 2% CSE (4 h) by cytochrome *c* reduction/xanthine-xanthine oxidase coupled assay. (*B*) Sod1-specific activity inhibited with the use of 1 mM diethyldithiocarbamate (DDC) in cell lysates of Wt MLF ($n = 3$) and KO-Rtp801 ($n = 3$) treated with 2% CSE (4 h). (*C*) Sod2-specific enzymatic activity remaining from Wt MLF ($n = 4$) and KO-Rtp801 ($n = 3$) treated with CSE (4 h) after incubation with DDC. (*D*) Total Gpx-specific activity of lysates of Wt MLF ($n = 4$) and KO-Rtp801 ($n = 3$) treated with 2% CSE (4 h). (*E*) Catalase-specific activity of lysates of MLF treated with 2% CSE (4 h). (*F*) Relative expression ($2^{-\Delta\Delta Ct}$) of antioxidant genes on Wt ($n = 4$) and KO-Rtp801 ($n = 3$) MLF incubated for 4 hours in 2% CSE. Data represent the average of at least three independent experiments performed in triplicate, and *error bars* indicate SD. Kruskal–Wallis significance, $^*P \leq 0.05$ or $^{**}P \leq 0.001$; ANOVA significance, $^*P \leq 0.05$ or $^{**}P \leq 0.001$ against untreated control cells in *F*. AntEnz, antioxidant enzyme; SA, specific activity.

which correlated to the decrease observed in MLF (Figure 7A). There were no significant differences in the basal gene expressions of *RTP801*, *SOD1*, *SOD2*, and *GPX1* antioxidant enzymes in primary human ATII cells from nonsmokers or moderate smokers or in ATII cells from G3-G4–characterized lungs (Figure 7B). Only the basal expression levels of the *CAT* gene were significant higher in ATII cells from G3-G4 lungs compared with nonsmoker control lungs. The expression of antioxidant enzymes in whole human lung lysates characterized as normal and COPD G0-G1, G2, and G3-G4 showed a significant decrease in *SOD2* expression only in G2 lungs. Interestingly, the levels of expression of *CAT* and *GPX1* genes were decreased in all the COPD-characterized lungs (Figure 7C).

Cellular Protection of Extracellular Antioxidant Enzymes in the Viability of MLF Exposed to Cigarette Smoke

We found extracellular superoxide dismutase activity in the culture medium of both control and 2% CSE–treated MLF (Figure E3A). We then investigated the viability of MLF after treatment with CSE in the presence of Sod, which produces H_2O_2 as a catalytic product. Because H_2O_2

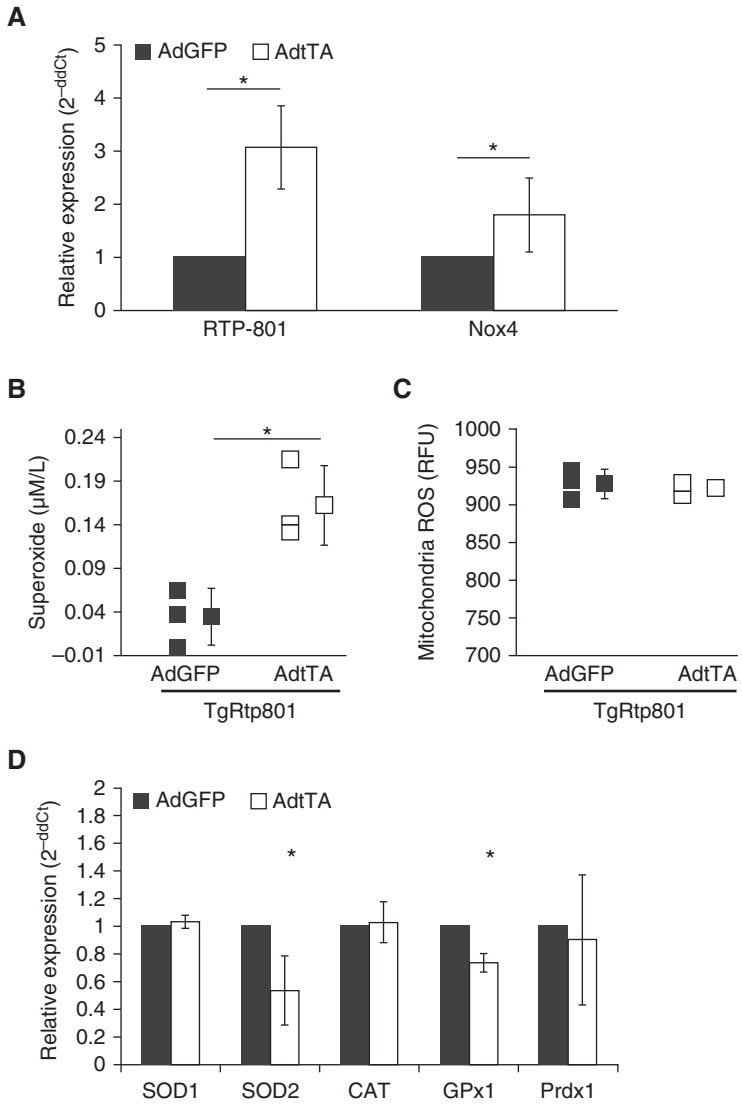

Figure 6. Overexpression of transgenic Rtp801in MLF shows similar effect of CSE induction of oxidative stress markers. The induction of Rtp801 expression was performed by transduction of 10^5 TgRtp801 MLF with 100 plaque-forming units per cell of the transactivator tet-off tTA-adenovirus (or CMV-GFP-adenovirus as control). (*A*) Rtp801 and Nox4 overexpression in TgRtp801 MLF after transduction with AdtTA ($n = 3$) and AdGFP control ($n = 3$). (*B*) Total superoxide production in TgRtp801 MLF after transduction with AdtTA ($n = 3$) and AdGFP control ($n = 3$) measured by cytochrome *c* reduction assay inhibitable by superoxide dismutase. (*C*) Mitochondria superoxide production in transactivated TgRtp801 MLF after transduction with AdtTA ($n = 3$) and AdGFP control ($n = 3$) measured by MitoSOX Red. (*D*) Relative expression ($2^{-\Delta\Delta Ct}$) of antioxidant genes on TgRtp801 MLF after transduction with AdtTA ($n = 3$) and AdGFP control ($n = 3$). Data represent the average of at least three independent experiments performed in triplicate, and *error bars* indicate SD. Kruskal–Wallis significance $^*P \leq 0.05$ against AdGFP transduced control. Ad, adenovirus; AdtTa, adenovirus transactivator; Tg, transgenic.

is cell permeable, it may be responsible for the observed decrease in cell viability. Accordingly, the addition of catalase aimed at eliminating H_2O_2 was predicted to improve cell viability after CSE treatment. Figure E3B shows the worsening effect of Sod on the viability of MLF treated for 4 hours with 2% CSE, which was reversed significantly by the presence of catalase. Moreover, Sod treatment alone did not change fluorescence in the MLF transduced with either Cyto-roGFP or Mito-roGFP probes when incubated with CSE (Figures 4C and 4D, respectively). In contrast, when the cells were incubated with CSE and Sod plus Cat, there was a significant decrease in the oxidation of the roGFP probes (Figures 4C and 4D).

Discussion

Every puff of TS contains thousands of reactive chemicals that ultimately cause oxidative and nitrosative stress (26). These compounds interact with endogenous sources of oxidants, including those originating from lung cells, potentially leading to lung cellular injury, a key determinant of COPD. Our data demonstrate that Rtp801, which is involved in suppressing mTOR signaling, was necessary and sufficient in amplifying the oxidative stress caused by TS. We found that this effect was mediated by activation of Nox4, causing increased production of cytoplasmic ROS, whereas there was a more modest participation of ROS originating from the mitochondria after up to 4 hours of CSE challenge. Moreover, cells expressing Rtp801 had decreased levels of antioxidants. On the other hand, we observed that KO-Rtp801 MLF had decreased ROS levels on exposure to CSE, accompanied by increased cell survival, which is largely supportive of our previous *in vivo* observations of protection of KO-Rtp801 mice from TS (9). The aggregate of these findings underscores the extent to which TS alters the cellular signaling involved in oxidant generation and antioxidant protection, largely involving Rtp801/mTOR signaling triggered by reactive oxidants present in TS.

To understand the amplification of the oxidative stress associated with the TS induction of Rtp801, we assessed the production of the superoxide radical. Our results showed significant extracellular (cytochrome *c* reduction inhibited by Sod) and intracellular (MitoSox Red) production of the radical superoxide in Rtp801 Wt MLF when treated with CSE. This superoxide production was associated with a decrease in cell viability and the induction of Rtp801. Using a cell-site–specific reporter probe, we determined that CSE-triggered ROS production was predominantly cytoplasmic rather than of mitochondria origin, which was largely supported by the cytoplasmic-extracellular (such as cytochrome *c* reduction and Cyto-roGFP probe) and the mitochondria-specific redox probes (such as MitoSox Red

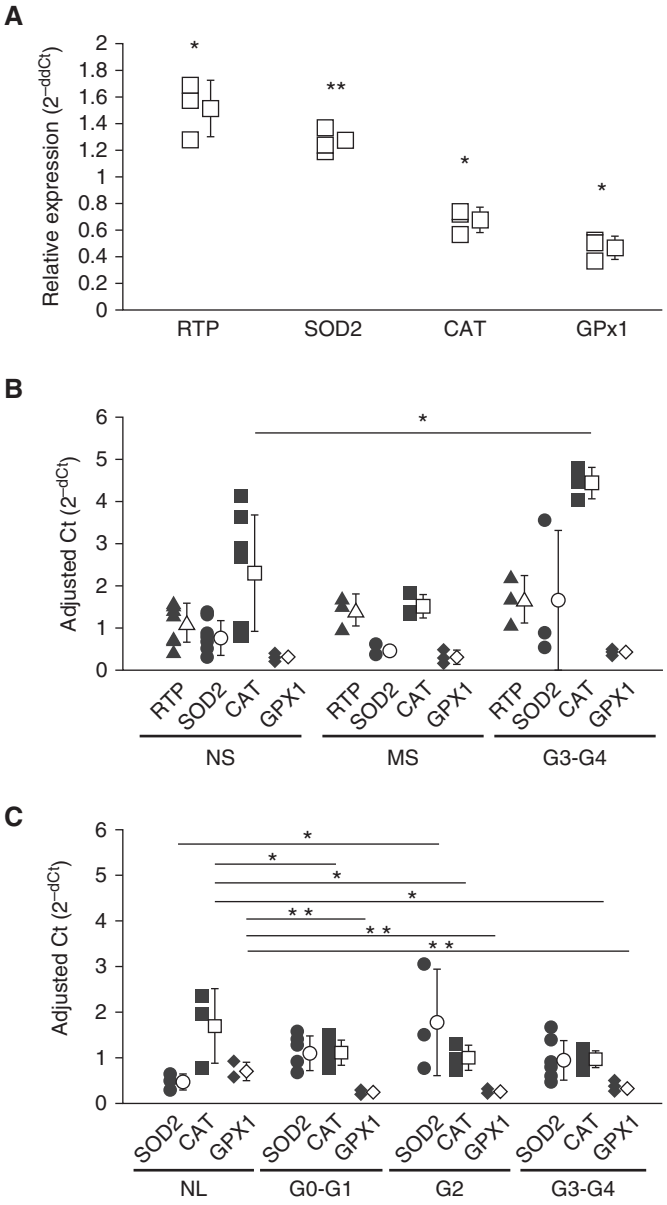

Figure 7. CSE and chronic obstructive pulmonary disease (COPD) status induces changes in the expression of antioxidant enzymes in human alveolar type II (ATII) cells and lungs. (*A*) Changes in RTP801 and antioxidant enzyme expression in primary human ATII cells from nonsmokers ($n = 3$) after treatment with 3% CSE for 4 hours (relative expression $2^{-\Delta\Delta Ct}$). (*B*) Basal RTP801 and antioxidant enzyme expression in primary human ATII cells from NS ($n = 6$), MS ($n = 6$), and G3-G4 ($n = 3$) characterized lungs. (*C*) Expression of antioxidant enzymes in human lungs characterized as NL ($n = 3$) and COPD G0-G1 ($n = 6$), G2 ($n = 3$), and G3-G4 ($n = 6$). Data represent the average of at least three independent experiments performed in triplicate, and *error bars* indicate SD. Kruskal–Wallis significance, $^{*}P \leq 0.05$ or $^{**}P \leq 0.001$ against untreated control cells in *A*; ANOVA significance, $^{*}P \leq 0.05$ or $^{**}P \leq 0.001$ against NS ATII cells in *B* and NL in *C*. Ct, cycle threshold; MS, moderate smokers; NL, normal lung; NS, nonsmoker.

and Mito-roGFP). These findings led us to focus on cytoplasmic sources of superoxide, which largely involve oxidases and oxygenases, including NADPH oxidase, xanthine oxidase, and lipoxygenase, among others.

Nox have been implicated largely in environmental responses associated with inflammation, because they produce superoxide anion and H_2O_2 (27). In the context of our studies, the potential Nox candidates for producing superoxide consist of Nox1, Nox2, Nox4, and Nox5 because they are the most commonly expressed Nox members in vascular cells.

In support of the contribution of Nox to the generation of CSE-induced oxidative stress, we observed a reduction in superoxide generation with the Nox inhibitor apocynin. Moreover, we found that the specific suppression of Nox4 transcript with siRNA significantly decreased the superoxide generation induced by CSE. These findings are consistent with the cytoplasmic redox changes detected with the compartment-specific oxidative stress probe Cyto-roGFP. Nox4 has been localized to focal adhesions, endoplasmic reticulum, nucleus, and mitochondria (27). Moreover, activation of Nox4 appears to require the translocation of Nox4 and p22phox to the plasma membrane, reflecting its activation and thus the production of extracellular superoxide. There is a growing evidence of stimulation of Nox4 by Akt (28–31), with the interaction with mTOR (32, 33), and perhaps by PKC after induction by TS (34). mTORC2 induction after mTORC1 inhibition is a possible mechanism of Nox4 activation mediated by Akt. In fact, activation of mTORC2 is redox sensitive (35). Moreover, Nox4 can also produce ROS released extracellularly (24). Our findings of extracellular Nox4-produced superoxide and the presence of extracellular Sod3 enzymatic activity in cells exposed to CSE may explain the production of H_2O_2, which might permeate back into the cells, as judged by the increase in the cytoplasmic redox measured by the Cyto-roGFP probe. In addition, Nox4 may enhance H_2O_2 production because of its superoxide dismutation activity (36). Altogether, this process further underscores its potential role in the enhancement of oxidative stress driven by Rtp801 after TS, linking this prototypic environmental stress with the Rtp801-mTOR-Nox4 axis.

In fact, Nox may play distinct roles in TS-induced inflammation. Neutrophil Nox2 appears to mediate protection against emphysema in mice exposed chronically to TS (37); furthermore, the decrease in Nox3 expression because of genetic deletion of Toll-like receptor 4 causes spontaneous emphysema in mice, underscoring Nox3's protective effect, because it is predominantly expressed by lung endothelial cells (38).

Oxidative stress involves an imbalance resulting from increased levels of oxidants and/or decreased cellular antioxidant defenses. To counteract the possible harmful effects of the superoxide anion, cells rely on antioxidant actions of the superoxide

dismutase family, acting in conjunction with catalase, Gpx, and peroxiredoxin, which reduce H_2O_2 formed during dismutation of superoxide. We observed a significant decrease in the total Sod activity in both Wt and KO-Rtp801 cells in response to the oxidative shift induced by CSE in MLF. Such low Sod levels were associated, in part, with an important reduction of Sod1 activity in both cell types (Figure 5B). However, Rtp801 Wt MLF had a more dramatic reduction in Sod2-specific activity and Sod2 expression caused by CSE. Extracellular Sod showed a small, nonsignificant increase in activity in Rtp801 Wt MLF after CSE incubation, which is related with the observed induction of the Sod3 gene. The increase of superoxide by Nox4 and its dismutation by Sod3 may account for the production of H_2O_2 and possible toxicity, if cytoplasmic catalase, Gpx, or peroxiredoxin are decreased in the cells. Furthermore, we found that Gpx enzymatic activity was induced more significantly only in KO-Rtp801 MLF after CSE treatment, with a lower level of induction in Wt MLF (Figure 5D), which may be related to a decrease in Gpx1 gene expression (Figure 5F). In addition, the expression of Prdx1 isoform was decreased in Rtp801 Wt cells after CSE treatment, probably accounting for the higher susceptibility of these cells to CSE-induced oxidative stress. The decrease in Sod activity after TS treatment has been documented in whole lung of mice (39) and rat alveolar macrophages (40) and in alveolar macrophages of elderly smokers (41). Conversely, overexpression of cytoplasmic Sod1 and extracellular Sod3 protects mice against TS-induced emphysema (42). In line with the protective role of SOD3 overexpression (43), there is one polymorphism in the SOD3 gene that correlates with the risk of emphysema (44).

There are important limitations in experimental studies of TS-induced COPD, including the differential response of rodent versus human cells, the specific behavior of the different structural alveolar cells (type I and II epithelial cells, endothelial cells, interstitial fibroblasts), and mild mouse lung disease-related phenotype when compared with human disease. Notwithstanding these limitations, few studies have focused on the pattern of expression of antioxidant enzymes in smokers' and COPD lungs and in experimental models of the disease. Importantly, we found that human ATII cells from patients with COPD have up-regulated RTP801 expression, a finding that is in line with our prior whole lung expression studies (9). Our finding of Gpx1 expression reduction in MLF can be extended to ATII cells from nonsmokers treated with CSE, and whole lungs from patients with COPD.

Conclusions

The results of this study support our proposed scheme of cellular TS-induced damage (Figure E3C). Rtp801 enhances the TS-induced oxidative stress by inhibiting mTORC1 and possibly activating mTORC2, which can phosphorylate Akt and PKC, thus enhancing Nox4 activity. The ROS produced by Nox4 in conjunction with the decrease in cellular antioxidant enzymatic defenses are responsible for the observed cytoplasmic redox changes and cellular damage. This investigation provides new and relevant insights into the role of the Rtp801-mTOR-Nox4 axis in the enhancement of TS-induced oxidative stress and cellular damage. ■

Author disclosures are available with the text of this article at www.atsjournals.org.

Acknowledgments: The authors thank Swapan Bose (University of Colorado School of Medicine, Aurora, CO) for his technical assistance and Paul Schumacker (Northwestern University, Feinberg School of Medicine, Chicago, IL), Brian B. Graham (University of Colorado School of Medicine, Aurora, CO), and Eric P. Schmidt (University of Colorado School of Medicine, Aurora, CO) for input into the final manuscript.

References

1. Alder JK, Guo N, Kembou F, Parry EM, Anderson CJ, Gorgy AI, Walsh MF, Sussan T, Biswal S, Mitzner W, *et al*. Telomere length is a determinant of emphysema susceptibility. *Am J Respir Crit Care Med* 2011;184: 904–912.
2. Tuder RM, Petrache I. Pathogenesis of chronic obstructive pulmonary disease. *J Clin Invest* 2012;122:2749–2755.
3. Yoshida T, Tuder RM. Pathobiology of cigarette smoke-induced chronic obstructive pulmonary disease. *Physiol Rev* 2007;87: 1047–1082.
4. Tsuji T, Aoshiba K, Nagai A. Alveolar cell senescence in patients with pulmonary emphysema. *Am J Respir Crit Care Med* 2006;174: 886–893.
5. Rangasamy T, Cho CY, Thimmulappa RK, Zhen L, Srisuma SS, Kensler TW, Yamamoto M, Petrache I, Tuder RM, Biswal S. Genetic ablation of Nrf2 enhances susceptibility to cigarette smoke-induced emphysema in mice. *J Clin Invest* 2004;114: 1248–1259.
6. Boutten A, Goven D, Artaud-Macari E, Boczkowski J, Bonay M. NRF2 targeting: a promising therapeutic strategy in chronic obstructive pulmonary disease. *Trends Mol Med* 2011;17:363–371.
7. Tuder RM, Yoshida T. Stress responses affecting homeostasis of the alveolar capillary unit. *Proc Am Thorac Soc* 2011;8:485–491.
8. Zoncu R, Efeyan A, Sabatini DM. mTOR: from growth signal integration to cancer, diabetes and ageing. *Nat Rev Mol Cell Biol* 2011;12:21–35.
9. Yoshida T, Mett I, Bhunia AK, Bowman J, Perez M, Zhang L, Gandjeva A, Zhen L, Chukwueke U, Mao T, *et al*. Rtp801, a suppressor of mTOR signaling, is an essential mediator of cigarette smoke-induced pulmonary injury and emphysema. *Nat Med* 2010;16:767–773.
10. DeYoung MP, Horak P, Sofer A, Sgroi D, Ellisen LW. Hypoxia regulates TSC1/2-mTOR signaling and tumor suppression through REDD1-mediated 14-3-3 shuttling. *Genes Dev* 2008;22:239–251.
11. Rennard SI. Inflammation and repair processes in chronic obstructive pulmonary disease. *Am J Respir Crit Care Med* 1999;160:S12–S16.
12. Waud WR, Brady FO, Wiley RD, Rajagopalan KV. A new purification procedure for bovine milk xanthine oxidase: effect of proteolysis on the subunit structure. *Arch Biochem Biophys* 1975;169:695–701.
13. Messier EM, Mason RJ, Kosmider B. Efficient and rapid isolation and purification of mouse alveolar type II epithelial cells. *Exp Lung Res* 2012;38:363–373.
14. Kosmider B, Messier EM, Chu HW, Mason RJ. Human alveolar epithelial cell injury induced by cigarette smoke. *PLoS One* 2011;6: e26059.
15. McCord JM, Fridovich I. The reduction of cytochrome c by milk xanthine oxidase. *J Biol Chem* 1968;243:5753–5760.
16. Bergmeyer HU. Measurement of catalase activity [in German]. *Biochem Z* 1955;327:255–258.
17. Lawrence RA, Burk RF. Glutathione peroxidase activity in selenium-deficient rat liver. 1976. *Biochem Biophys Res Commun* 2012;425: 503–509.
18. Lowry OH, Rosebrough NJ, Farr AL, Randall RJ. Protein measurement with the Folin phenol reagent. *J Biol Chem* 1951;193:265–275.
19. Waypa GB, Schumacker PT. Hypoxia-induced changes in pulmonary and systemic vascular resistance: where is the O_2 sensor? *Respir Physiol Neurobiol* 2010;174:201–211.
20. Nadon AM, Perez MJ, Hernandez-Saavedra D, Smith LP, Yang Y, Sanders LA, Gandjeva A, Chabon J, Koyanagi DE, Graham BB, *et al*. Rtp801 suppression of epithelial mTORC1 augments endotoxin-induced lung inflammation. *Am J Pathol* 2014;184:2382–2389.

21. Su Y, Han W, Giraldo C, De Li Y, Block ER. Effect of cigarette smoke extract on nitric oxide synthase in pulmonary artery endothelial cells. *Am J Respir Cell Mol Biol* 1998;19:819–825.
22. Brugarolas J, Lei K, Hurley RL, Manning BD, Reiling JH, Hafen E, Witters LA, Ellisen LW, Kaelin WG Jr. Regulation of mTOR function in response to hypoxia by REDD1 and the TSC1/TSC2 tumor suppressor complex. *Genes Dev* 2004;18:2893–2904.
23. Brugarolas JB, Vazquez F, Reddy A, Sellers WR, Kaelin WG Jr. TSC2 regulates VEGF through mTOR-dependent and -independent pathways. *Cancer Cell* 2003;4:147–158.
24. von Löhneysen K, Noack D, Wood MR, Friedman JS, Knaus UG. Structural insights into Nox4 and Nox2: motifs involved in function and cellular localization. *Mol Cell Biol* 2010;30:961–975.
25. Messier EM, Bahmed K, Tuder RM, Chu HW, Bowler RP, Kosmider B. Trolox contributes to Nrf2-mediated protection of human and murine primary alveolar type II cells from injury by cigarette smoke. *Cell Death Dis* 2013;4:e573.
26. Rahman I, Adcock IM. Oxidative stress and redox regulation of lung inflammation in COPD. *Eur Respir J* 2006;28:219–242.
27. Al Ghouleh I, Khoo NK, Knaus UG, Griendling KK, Touyz RM, Thannickal VJ, Barchowsky A, Nauseef WM, Kelley EE, Bauer PM, *et al*. Oxidases and peroxidases in cardiovascular and lung disease: new concepts in reactive oxygen species signaling. *Free Radic Biol Med* 2011;51:1271–1288.
28. Ismail S, Sturrock A, Wu P, Cahill B, Norman K, Huecksteadt T, Sanders K, Kennedy T, Hoidal J. NOX4 mediates hypoxia-induced proliferation of human pulmonary artery smooth muscle cells: the role of autocrine production of transforming growth factor-beta1 and insulin-like growth factor binding protein-3. *Am J Physiol Lung Cell Mol Physiol* 2009;296:L489–L499.
29. Gibberd FB, Blair JA, Parveen H, Barford PA, Leeming RJ. Aetiology of Parkinson's disease. *The Lancet* 1984;323:167.
30. Park S, Ahn JY, Lim MJ, Kim MH, Yun YS, Jeong G, Song JY. Sustained expression of NADPH oxidase 4 by p38 MAPK-Akt signaling potentiates radiation-induced differentiation of lung fibroblasts. *J Mol Med (Berl)* 2010;88:807–816.
31. Peng H, Li W, Seth DM, Nair AR, Francis J, Feng Y. (Pro)renin receptor mediates both angiotensin II-dependent and -independent oxidative stress in neuronal cells. *PLoS One* 2013;8:e58339.
32. Kato H, Nakajima S, Saito Y, Takahashi S, Katoh R, Kitamura M. mTORC1 serves ER stress-triggered apoptosis via selective activation of the IRE1-JNK pathway. *Cell Death Differ* 2012;19:310–320.
33. Eid AA, Ford BM, Bhandary B, de Cassia Cavaglieri R, Block K, Barnes JL, Gorin Y, Choudhury GG, Abboud HE. Mammalian target of rapamycin regulates Nox4-mediated podocyte depletion in diabetic renal injury. *Diabetes* 2013;62:2935–2947.
34. Asano H, Horinouchi T, Mai Y, Sawada O, Fujii S, Nishiya T, Minami M, Katayama T, Iwanaga T, Terada K, *et al*. Nicotine- and tar-free cigarette smoke induces cell damage through reactive oxygen species newly generated by PKC-dependent activation of NADPH oxidase. *J Pharmacol Sci* 2012;118:275–287.
35. Nayak BK, Feliers D, Sudarshan S, Friedrichs WE, Day RT, New DD, Fitzgerald JP, Eid A, Denapoli T, Parekh DJ, *et al*. Stabilization of HIF-2α through redox regulation of mTORC2 activation and initiation of mRNA translation. *Oncogene* 2013;32:3147–3155.
36. Takac I, Schröder K, Zhang L, Lardy B, Anilkumar N, Lambeth JD, Shah AM, Morel F, Brandes RP. The E-loop is involved in hydrogen peroxide formation by the NADPH oxidase Nox4. *J Biol Chem* 2011; 286:13304–13313.
37. Yao H, Edirisinghe I, Yang SR, Rajendrasozhan S, Kode A, Caito S, Adenuga D, Rahman I. Genetic ablation of NADPH oxidase enhances susceptibility to cigarette smoke-induced lung inflammation and emphysema in mice. *Am J Pathol* 2008;172:1222–1237.
38. Zhang X, Shan P, Jiang G, Cohn L, Lee PJ. Toll-like receptor 4 deficiency causes pulmonary emphysema. *J Clin Invest* 2006;116: 3050–3059.
39. Bai X, Chen Y, Chen W, Lei H, Gao F, Qin Y, Zheng J, Shi G. The effect of black coral extraction on acute lung inflammation induced by cigarette smoke in mice. *Exp Lung Res* 2011;37:627–632.
40. Pires KM, Lanzetti M, Rueff-Barroso CR, Castro P, Abrahão A, Koatz VL, Valença SS, Porto LC. Oxidative damage in alveolar macrophages exposed to cigarette smoke extract and participation of nitric oxide in redox balance. *Toxicol In Vitro* 2012; 26:791–798.
41. Kondo T, Tagami S, Yoshioka A, Nishimura M, Kawakami Y. Current smoking of elderly men reduces antioxidants in alveolar macrophages. *Am J Respir Crit Care Med* 1994;149:178–182.
42. Foronjy RF, Mirochnitchenko O, Propokenko O, Lemaitre V, Jia Y, Inouye M, Okada Y, D'Armiento JM. Superoxide dismutase expression attenuates cigarette smoke- or elastase-generated emphysema in mice. *Am J Respir Crit Care Med* 2006;173:623–631.
43. Yao H, Arunachalam G, Hwang JW, Chung S, Sundar IK, Kinnula VL, Crapo JD, Rahman I. Extracellular superoxide dismutase protects against pulmonary emphysema by attenuating oxidative fragmentation of ECM. *Proc Natl Acad Sci USA* 2010;107: 15571–15576.
44. Sørheim IC, DeMeo DL, Washko G, Litonjua A, Sparrow D, Bowler R, Bakke P, Pillai SG, Coxson HO, Lomas DA, *et al*.; International COPD Genetics Network Investigators. Polymorphisms in the superoxide dismutase-3 gene are associated with emphysema in COPD. *COPD* 2010;7:262–268.